Polymer selection impacts the pharmaceutical profile of site specifically conjugated Interferon-α2a

Niklas Hauptstein[a]‡, Paria Pouyan[b]‡, Kevin Wittwer[c], Gizem Cinar[d,e], Oliver Scherf-Clavel[a], Martina Raschig[a], Kai Licha[b], Tessa Lühmann[a], Ivo Nischang[d,e], Ulrich S. Schubert[d,e], Christian Pfaller[c], Rainer Haag[b], Lorenz Meinel*[a,f]

[a] Institute of Pharmacy and Food Chemistry, University of Würzburg, Am Hubland, 97074 Würzburg Germany

[b] Institute of Chemistry and Biochemistry, Freie Universität Berlin, Takustr. 3, 14195 Berlin Germany

[c] Paul-Ehrlich-Institute, Division of Veterinary Medicine, Paul-Ehrlich-Str. 51-59, 63225 Langen, Germany

[d] Laboratory of Organic and Macromolecular Chemistry (IOMC), Friedrich Schiller University Jena, Humboldtstr. 10, 07743 Jena, Germany

[e] Jena Center for Soft Matter (JCSM), Friedrich Schiller University Jena, Philosophenweg 7, 07743 Jena, Germany

[f] Helmholtz Institute for RNA-Based Infection Research (HIRI), 97080 Würzburg, Germany

‡ These authors contributed equally to this work

Keywords: bioconjugate; genetic code expansion; polyglycerol; poly(ethylene glycol); analytical ultracentrifugation; pharmacokinetic

To whom correspondence should be addressed:

Prof. Dr. Dr. Lorenz Meinel, Institute of Pharmacy and Food Chemistry, University of Würzburg, Am Hubland, DE-97074 Würzburg, Germany, lorenz.meinel@uni-wuerzburg.de, Tel.: +49 931 3185471

Highlights

- IFN-α2a bioconjugates with linear polyglycerols (LPG) and linear PEGs were designed.
- Pharmacokinetics of the 40 kDa PEG- IFN-α2a matched the marketed product, Pegasys.
- LPG-IFN-α2a had faster disposition kinetics in spite of comparable radii as compared to PEG-IFN-α2a.
- Therefore, the study points to an expanded polymer design space for bioconjugate synthesis.

Abstract

Conjugation of poly(ethylene glycol) (PEG) to biologics is a successful strategy to favorably impact the pharmacokinetics and efficacy of the resulting bioconjugate. We compare bioconjugates synthesized by strain-promoted azide-alkyne cycloaddition (SPAAC) using PEG and linear polyglycerol (LPG) of about 20 kDa or 40 kDa, respectively, with an azido functionalized human Interferon-α2a (IFN-α2a) mutant. Site specific PEGylation and LPGylation resulted in IFN-α2a bioconjugates with improved *in vitro* potency as compared to commercial Pegasys. LPGylated bioconjugates had faster disposition kinetics despite comparable hydrodynamic radii to their PEGylated analogues. Overall exposure of the PEGylated IFN-α2a with a 40 kDa polymer exceeded Pegasys which, in return, was comparable to the 40 kDa LPGylated conjugates. The study points to an expanded polymer design space by means of which the selected polymer class may result in different distribution of the studied bioconjugates.

Introduction

PEGylation, the attachment of poly(ethylene glycol) (PEG) to a biologic, may improve various pharmaceutical aspects of the resulting bioconjugates, including stability, solubility, and pharmacokinetics [1-3]. PEGylation increases a drug's hydrodynamic volume and may, at proper overall size, reduce drug disposition by decreasing glomerular filtration [4, 5]. Another aspect of PEG known as "stealth-effect", shields PEGylated biologics in part from phagocytic cells, thereby reducing elimination [1, 2]. Both aspects contribute to longer half-lives, and have been reported for PEGylated Interferon-α2a (IFN-α2a), which is the starting point of our study [6, 7]. IFN-α2a, a cytokine with potent, antiviral, immune-modulating and antiproliferative properties, is used for hepatitis and cancer therapy since the 1980's [8]. We selected IFN-α2a for its wealth of available information [6-21]. Today IFN-α2a is marketed as a PEGylated biologic: One IFN-α2a carrying a 40 kDa branched PEGs (Pegasys)[21, 22], one IFN-α2a carrying a12 kDa linear PEG (PEGIntron)[23], or one IFN-α2a carrying a branched 40 kDa PEG which is N-terminally linked (Besremi) [24].

To date, there are more than 20 FDA approved PEGylated proteins and drugs on the market [25]. These PEGylated bioconjugates are challenged by at least two aspects, firstly, the missing control of the modification site at the biologic and secondly, immunological challenges regarding PEG [26-29]. Concerning the first aspect, many of the existing products may further improve their current chemical ligation strategies for reproducible product qualities and better yields. Site specific strategies pointing in this direction include the use of cysteines, tyrosines, arginines, or the N- and C-terminus; these have been nicely reviewed elsewhere [30]. However, as of today, many products failed along these lines, resulting in heterogeneous product mixtures.

Consequently, rigorous fractionation of the heterogeneous bulk is required during purification to isolate the desired fractions. More recently, biologics have been introduced facilitating site-specific enzymatic catalysis, an approach which uses a biologic's intrinsic substrate site or, if not available, a genetically introduced substrate site through which functionalized polymers are enzymatically conjugated [31-35]. Alternatively, genetical introduction of unnatural amino acids, guarantees polymer decoration at that preselected site [36-52]. As to the second, immunological challenges of PEGylated biologics, recent reports point to possible side-effects including hypersensitivity,[53, 54] and immunological responses,[28, 55] which are at least in part driving accelerated plasma clearance after repetitive dosing [56]. Hence, expanding the polymer space beyond PEGylation is of much interest and linear polyglycerol (LPG) has been discussed in this context before [49, 51, 52].

Therefore, we recently synthesized bioconjugates through strain-promoted azide-alkyne cycloaddition (SPAAC), starting off a genetically engineered, azido-IFN-α2a mutant and functionalized PEG, and LPG polymers of about 10 kDa, respectively [49]. All products were generally comparable across the two polymer chemistries reported here, including their preferential interaction sites with the protein-surface. We are now expanding to bioconjugates with higher polymer molecular weights of about 20 and 40 kDa as required for a therapeutically relevant half-life and compare the outcome to the commercial PEGylated IFN-α2a bioconjugate, Pegasys [21, 22].

Materials and methods

Materials. Boc-protected L-lysine was from P3 BioSystems LLC (Shelbyville, KY). 2-bromoethanol, triphosgene, sodium azide, HCl in diethyl ether ($c = 2\ mol \cdot L^{-1}$), 1,4-dithiothreitol (DTT), carbenicillin, chlorampenical, isopropyl-β-D-thiogalactopyranosid (IPTG), penicillin-streptomycin, phenylmethylsulfonyl fluoride (PMSF), guanidine hydrochloride, primer, NDSB-201, L-(+)-arabinose, lysozyme, DNAse I, triton X-100, acetonitrile HPLC grade, ethylacetate, trifluoracetic acid, human plasma, phosphate buffered saline (PBS), potassium phthalimide (99%), hydrazine monohydrate (64-65% N_2H_4, 98%), (1*R*,8*S*,9s)-bicyclo[6.1.0]non-4-yn-9-ylmethyl *N*-succinimidyl carbonate (BCN-NHS), dichloromethane (anhydrous, ≥ 99.8%), and triethylamine (anhydrous, ≥ 99%) were purchased from Sigma Aldrich (Schnelldorf, Germany). PageRuler™ Prestained Protein Ladder, PageRuler™ Unstained Broad Range Protein Ladder, Coomassie Brilliant Blue G250, slide-a-Lyzer, Dulbecco's Modified Eagle's Medium (DMEM), Gibco-FBS-HI (Origin Brasil), BCA assay, synthesized IFN-α2a genes, *E. coli* BL21(DE3) Star bacteria, MagicMedia™ *E. coli* Expression Medium, Pierce C18 Tips, SYPRO™ Orange Protein Gel Stain, IFN-α Human Instant ELISA™ Kit (BMS216INST) were received from Thermo Fisher Scientific Germany (Darmstadt, Germany). BioPro IEX SmartSep S20 1 mL and 5 mL were obtained from YMC Europe (Dinslaken, Germany). XK16/600 Superdex 75 pg column was received from Cytiva Life Sciences (Freiburg, Germany). Zorbax 300SB-CN column was ordered from Agilent (Waldbronn, Germany). Vivaspin centrifugal concentrators were obtained from Sartorius AG (Göttingen, Germany). Spectra/Por 1 Dialysis Membrane Standard RC tubing was ordered from Repligen (Ravensburg, Germany). ROTIPHORESE® NF-Acrylamide/Bis-Solution 30 (29:1) was obtained from Carl Roth GmbH (Karlsruhe, Germany). HEK-Blue™ IFN-

α/β Cells, blasticidin and zeocin were ordered from Invivogen (Toulouse, France). Bovine serum albumin standard for MALDI-MS calibration was purchased from Bruker (Bremen, Germany).

Synthesis of polymers. Polymer synthesis of LPG and PEG was performed as described previously [49]. In brief, LPG was synthesized by monomer-activated anionic ring-opening polymerization. Prior to polymerization, the glycidols' hydroxyl groups were protected by acetal groups, which were removed in acidic media afterward, yielding the linear deprotected backbone. For functionalization, the terminal bromide group was reduced to an amine and functionalized using BCN-NHS, yielding the terminally functionalized LPG. PEG was bought as PEG-amine and directly functionalized with BCN-NHS.

Analytical ultracentrifugation. A stock solution of each polymer was prepared and diluted with water to obtain concentrations of approximately 0.25 mg mL^{-1} and 0.75 mg mL^{-1}, respectively. The aqueous solutions of the protein IFNK31N_3 and the bioconjugates were diluted with 10 mM phosphate-buffered saline (PBS, pH = 7.4) to obtain a sample concentration of approximately 0.75 mg mL^{-1}. Sedimentation velocity experiments were performed with an Optima Analytical Ultracentrifuge (Beckman Coulter Instruments, Brea, CA) by utilizing double-sector Epon centerpieces with a 12 mm solution optical path length. The cells were placed in an An-50 Ti eight-hole rotor. The cells were filled with 420 µL sample solution in diluent and with 440 µL water (polymers) or water / PBS buffer (10 mM) mixture (IFNK31N_3 and bioconjugates) as the reference. All samples were measured by using the interference optical detection module (refractive index (RI)) for observation of sedimentation boundaries in respect to time. For the protein and bioconjugates, additionally the absorbance detection module at λ = 280 nm was used. All measurements were performed at 20 °C and at a rotor speed of 42 000 rpm for up to 48 hours, depending on the sample. A three-minute (polymers) or five-minute (IFNK31N_3 and

bioconjugates) time interval between each scan was used. Analysis of a suitable selection of scans was used for data evaluation with Sedfit [57]. Viscosity and density measurements of the solvents were performed at the accurate compositions utilized for the experiments with a DMA4100 densimeter (Anton Paar, Graz, Austria) at 20 °C. For viscosity measurements of the exact same solvents, an Automated Microviscometer (AMVn, Anton Paar, Graz, Austria) at 20 °C was used (**Table S1**). The instrument was operated with a capillary / ball combination. Sedimentation velocity analytical ultracentrifugation (AUC) data were evaluated by numerical solution of the Lamm equation via Sedfit making use of the c(*s*) model, returning differential distributions of sedimentation coefficients, *s*, and weight average translational frictional ratios, f/f_{sph} [57, 58]. Here, f is the translational friction coefficient of the investigated macromolecules and f_{sph} the translational friction coefficient of a spherical particle with the same anhydrous volume and mass [59]. Numerical estimates of signal (weight) average values of s and the f/f_{sph} values from sedimentation-diffusion analysis are summarized in Table S2. The used partial specific volumes, υ, for the c(*s*) model, allowing numerical solution of the Lamm equation, were taken from the literature (υ = 0.83 cm^3 g^{-1} for PEGs)[59, 60]. For the LPG polymers, a partial specific volume of υ = 0.73 cm^3 g^{-1} was taken based on unpublished previous experimental results. For the IFNK31N$_3$, we utilized a typical value for proteins (υ = 0.73 cm^3 g^{-1}) as reported in the literature [61, 62], and also in line with previous studies of a related protein [63]. υ for the PEG conjugate was calculated by use of υ of PEGs and the protein weighed by mass fractions of components in the conjugate (as known from separate AUC investigations of PEG polymer and protein), resulting in υ = 0.76 cm^3 g^{-1}. υ for the LPGs and protein had similar values and, therefore, were also taken for the conjugate (υ = 0.73 cm^3 g^{-1}). The intrinsic sedimentation coefficients, *[s]*, were calculated by $[s] = s\eta_0/(1-\upsilon\rho_0)$ with the solvent viscosity, η_0, and solvent density, ρ_0. Molecular weights by AUC (**Table S2**)

were calculated from the lowest investigated polymer concentration being closest to solution ideality by utilizing the modified Svedberg equation: $M_{s,f} = 9\pi\sqrt{2}N_A([s](f/f_{sph}))^{3/2}\sqrt{v}$ with N_A being the Avogadro constant [59, 60].

Size exclusion chromatography of polymers. Size exclusion chromatography (SEC) of polymers was performed as described previously [49]. In brief, SEC of LPG polymers was performed in pure water with an Agilent 1100 SEC system (Agilent Technologies, Santa Clara, CA, USA), equipped with an automatic injector, isocratic pump and an Agilent 1100 diffractometer. As a column, a PSS Suprema column (pre-column, 1x with pore size of 30 Å, 2x with pore size of 1000 Å, all of them with a particle size of 10 µm) was used with a flow rate of 1 mL/min. Calibration was performed with pullulan standards prior to measurements. Molecular weight of the PEG used for conjugation was taken as provided by the manufacturer.

Expression and purification of IFN-α2a and mutant. Expression of IFN-α2a and IFNK31N_3 was performed as described before [49]. In brief, expression was in *E. Coli* (BL21) DE3 bacteria with IPTG induction. For the mutant, expression of the pyrrolysyl-tRNA synthethase/$tRNA^{Pyl}$ CUA pair was done by co-induction with L(+)-arabinose of a pEVOL-pylRS vector containing a chloramphenicol resistance cassette, which was kindly donated by Prof. Dr. Edward A. Lemke from the Johannes Gutenberg University of Mainz/EMBL Heidelberg [64, 65]. After expression, inclusion bodies were isolated and refolded. The refolded protein was purified by anion and cation exchange chromatography, followed by SEC.

Strain promoted azide-alkyne Huisgen cyclo-addition. Strain promoted azide-alkyne Huisgen cyclo-addition (SPAAC) was performed as described previously [49]. In brief, the protein was mixed with a 20-fold excess of polymer in 25 mM phosphate buffer pH 7.4 + 150 mM NaCl at a

concentration of approximately 500 µg/mL and incubated for 48 h under gentle stirring at 4 °C in a borosilicate glass vessel. For the 40 kDa polymers, the SPAAC reaction was allowed for a timescale of 72 h.

Sodium dodecyl sulphate polyacrylamide gel electrophoresis. Sodium dodecyl sulphate polyacrylamide gel electrophoresis (SDS-PAGE) was performed as described previously using standard Tris-glycine buffer systems. For samples with a molecular weight up to 40 kDa (up to 20 kDa bioconjugates) 10 to 15% SDS-Gels were used. For samples with a molecular weight above 40 kDa 5 to 15 % SDS-Gels were used.

Reversed phase high pressure liquid chromatography analysis. Reversed phase high pressure liquid chromatography (RP-HPLC) analysis was performed as described prevously[49]. In brief, an Agilent Zorbax 300SB-CN (4.6 x 150 mm, 5 µm particle) column was used for analysis, using a linear gradient of 5 to 70% eluent B (%, v/v) within 35 min at a constant flow of 1 mL/min. Eluent A = Water + 0.1% TFA and eluent B = ACN + 0.1% TFA, λ = 214 nm.

Dynamic light scattering. Dynamic light scattering (DLS) was performed as described previously with adaptions [66]. DLS was performed on a Malvern Zetasizer ZS (Malvern Panalytical, Herrenberg, Germany). Measurements were performed at 25 °C in 100 mM phosphate buffer pH 7.2 + 150 mM NaCl (c[Protein] = 0.4 mg/mL) after sterile filtration. Three measurements were performed of each sample, whereby three acquisitions were averaged per measurement. Results are reported as intensity value as shown in the Zetasizer software (version 7.13).

HEK Blue IFNα/β cell culture assay. The cell culture assay was performed in HEK-Blue™ IFN-α/β cells according to the manufacturer's instructions. In brief, 50 000 cells were seeded at day 1 in a 96-well plate (280 000 cells/mL) in each well and stimulated with IFN bioconjugates starting

at a concentration of 1 µg/mL, followed by eleven 10-fold dilutions. On day 2, 20 µL of the supernatants were mixed with 180 µL of Quanti-Blue™ and analyzed at λ = 630 nm after 120 min of incubation at 37 °C. The potency of 10 kDa bioconjugates was reported previously [49] and were measured again on the same plates here along with the other molecular weight bioconjugates for comparability purposes.

Differential scanning fluorimetry. Differential scanning fluorimetry (DSF) was performed as described previously [49]. In brief, bioconjugates were analyzed at a final concentration of 8 µM protein equivalents over a range of 25 to 95 °C using a heating ramp of 1 °C/min, whereby SYPRO Orange was used at a 5-fold concentration. Normalization was performed as described before, without smoothing of data [67].

***In vivo* pharmacokinetic study in mice.** Animal experiments were carried out in compliance with the regulations of the German animal protection laws and authorized by the responsible state authority (Regierungspräsidium Darmstadt, Dezernat V54 - Veterinärwesen und Verbraucherschutz). Male and female transgenic C57BL/6 B6.Tg(ISRE-eGFP)Tovey mice [68] between 8 and 18 weeks of age were divided into groups of 15 animals for each interferon conjugate (mean group age 10 to 13 weeks). Mice were weighed, interferon conjugates were diluted in sterile PBS and 3 µg/kg bodyweight of IFN-α2a-WT equivalents (therefore the protein amount was always the same) of the respective dilution were administered intravenously in the tail vein. For blood sampling, groups were divided into three subgroups of five animals each. In each subgroup, blood was taken at two time points, respectively (time points 1+4, 2+5, 3+6 as reported in **Scheme 1**). At the first time point, mice were anesthetized using isoflurane, and 100 µL blood was taken from the retro-orbital vein plexus. At the second time point, animals were anesthetized by intraperitoneal injection of Ketamine/Xylazine (100 mg/10 mg per kg bodyweight) and

exsanguinated via cardiac heart puncture. Serum was obtained by blood centrifugation at 14.000 x g at 4 °C for 10 min. The serum was then snap-frozen in liquid nitrogen, followed by storage at -80 °C until further analysis. After thawing on ice, the collected serum samples were diluted appropriately and analyzed by ELISA (see below for details) according to the manufacturer's instructions. The primary data set was fitted using non-linear least squares fits using RStudio (version 4.0.5) [69].

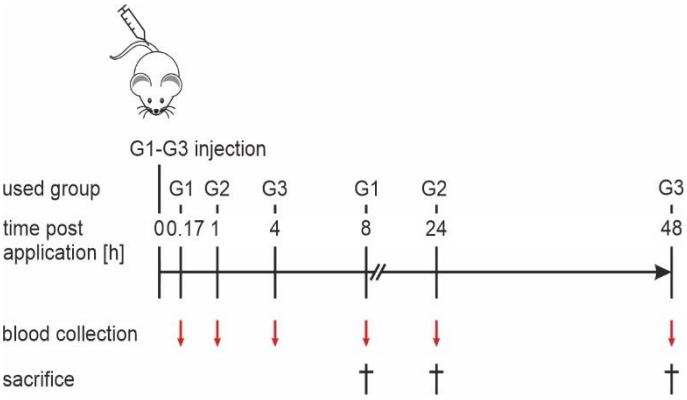

Scheme1: Protocol of the *in vivo* pharmacokinetic study.
G1= group 1, G2 = group 2, G3 = group 3 (n = 5).

Plasma stability of Interferon-α2a and bioconjugates. IFN-α2a WT and its bioconjugates were spiked into plasma to a final concentration of 1 ng/mL. The plasma was incubated at 37 °C at 300 rpm for up to 48 h. Samples were taken at 0,1,3,7,24, and 48 h and snap frozen in liquid nitrogen until further analysis. IFN concentrations of the samples were analyzed by ELISA (see below for details) setting the averaged concentration of IFN-α2a WT at 0 h as the 100% reference.

Enzyme-linked immunosorbent assay. Samples of plasma stability and serum samples from the *in vivo* pharmacokinetic study were analyzed by enzyme-linked immunosorbent assay (ELISA). Samples taken for plasma stability were directly used. Samples taken from the *in vivo* study were

25-fold diluted using the kits dilution buffer, except from IFN-α2a WT, setting the maximum expected concentration to 2 ng/mL. IFN-α2a WT was only diluted 2-fold as an initial trial did show too low detectable concentrations indicating a rapid decay. To account for polymer specific decreased antibody binding, every bioconjugate, as well as the WT was analyzed with a calibration curve established by the pure bioconjugate as the reference. For the calibration curve, the same concentrations were used as the supplied standard calibration concentrations (39 to 2500 pg/mL+ blank). The lower limit of detection was 3.3 pg/mL, according to the manufacturer.

Stimulation of B6.Tg(ISRE-eGFP) Tovey mice bone marrow cells followed by fluorescent activated cell sorting analysis. Animals were sacrificed by intraperitoneal anesthesia (Ketamine/Xylazine (100 mg/10 mg per kg bodyweight)) and exsanguination. Femoral bones were dissected, flushed with RPMI (10% FBS, 1% L-glutamine, 1% P/S, 1% Na-pyruvate) and 10^6 bone marrow cells were seeded in a 24-well plate. Human IFN-α2a WT (1000 ng/ml) or murine IFN-α2a WT (1000 U/ml) was added and plates were incubated for 24 hours at 37°C. The next day, cells were washed twice with PBS (1% FBS, 0.1% NaN_3). PBS supplemented with 1% paraformaldehyde was used to re-suspend the cell pellet and GFP expression was determined using a CytoFLEX flow cytometer (Beckman Coulter, Krefeld, Germany).

Statistical analysis. Statistical analysis was performed with Graphpad Prism 6. Results were compared by one-sided ANOVA, followed by Tukey *post hoc* test for pair-wise comparison; $p < 0.05$ was considered statistically significant.

Results

Polymer synthesis and characterization

The synthesis of PEG and LPG polymers started off previous protocols with adaptations as required for the longer polymer chains (**Figures 1A, B, Scheme S1, Figures S1-3**)[49, 70]. LPG was synthesized by anionic ring-opening polymerization of the acetal protected glycerol with $(Oct)_4NBr$ in toluene in presence of $(i\text{-}Bu)_3Al$ as activator (**Scheme S1**). After polymerization, the acetal protected backbone was treated in slightly acidic media and the respective LPG with free hydroxyl moieties was obtained (data not shown)[49]. To introduce the cyclooctyne group for SPAAC, the bromide at the chain-end was substituted with an azide group with NaN_3 (data not shown)[49]. In a subsequent step, the azide was reduced to a primary amine which was then modified with BCN-NHS (**Figure S1**). SEC measurements confirmed LPG polymers with similar molecular weights to theoretical values (**Figure S2, Table 1**). The commercial PEG-NH_2 was modified with BCN-NHS and analogous to the synthesis with LPG-NH_2 (**Figure S3**).

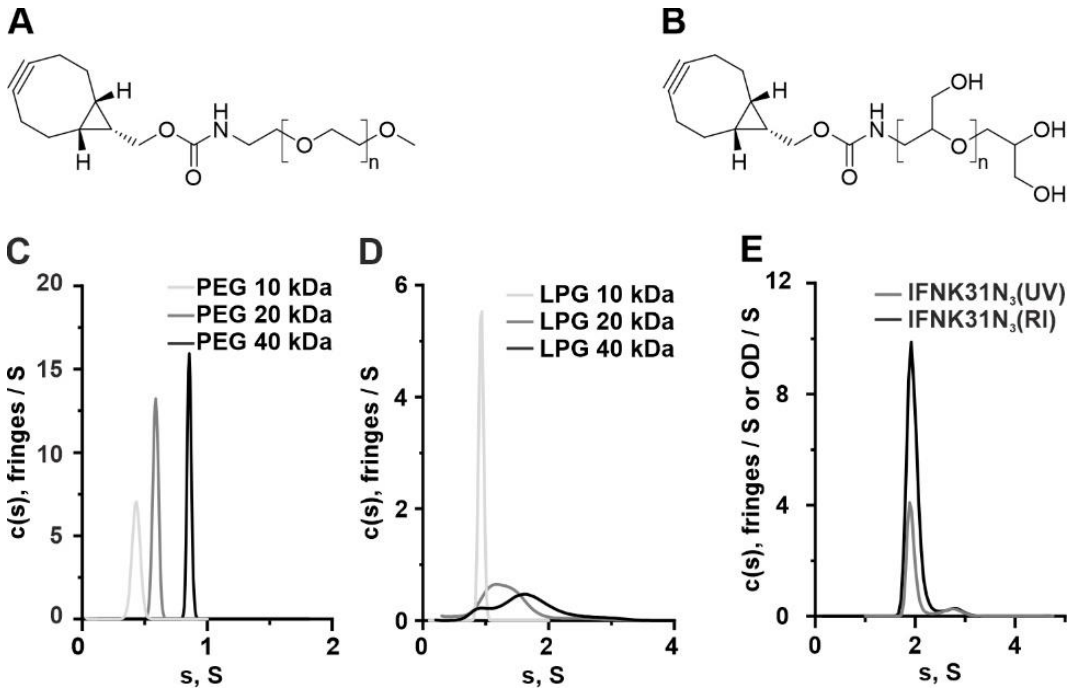

Figure 1: (A) Chemical structure of BCN-PEG and (B) BCN-LPG. Differential distributions of sedimentation coefficients, c(*s*), of (C) NH_2-PEG polymers (c ≈ 0.26 mg mL^{-1}), (D) N_3-LPG polymers (c ≈ 0.25 mg mL^{-1}) of different molecular weights, and (E) $IFNK31N_3$ (c ≈ 0.75 mg mL^{-1}). The latter results were obtained from RI (in terms of interference fringes) and absorbance detection (in terms of optical density (OD) at λ = 280 nm). AUC measurements and evaluation of polymers that are displayed in C and D were also performed at a higher concentration, results which are displayed in Figure S4.

All polymers were characterized by AUC as amino-, or as azide intermediates (**Scheme S1, Tables 1, S2, Figures 1C, D, S4**) and by SEC for comparison (**Table 1, Figure S2**). Results from both analyses were in the same order of magnitude with lower apparent molecular weight values obtained by AUC as compared to calibrated SEC against standards, an aspect not surprising concerning previous studies [59, 60]. The sedimentation coefficients, *s*, and translational frictional ratios, f/f_{sph}, from sedimentation-diffusion analysis for PEG were in agreement with a more detailed previous report (**Table S2**)[59]. The larger LPGs had broader differential distributions of sedimentation coefficients, c(*s*), as compared to PEG (**Figure 1C and D, S4A-C**). Within the row of increased molecular weights of LPGs, a clear increase in dispersity is seen. The signal (weight) average sedimentation coefficients, *s*, obtained by integration of the differential distributions,

increased from *s* = 0.43 S (Svedberg) to *s* = 0.59 S and *s* = 0.86 S for the 10 kDa, 20 kDa, and 40 kDa PEG (**Figures 1D, S6, Table S2**), and from *s* = 0.93 S to *s* = 1.35 S and *s* = 1.66 S for the10 kDa, 20 kDa, and 40 kDa LPGs (**Figures 1C and D, S4, Table S2**).

Table 1: Polymer characterization by SEC, AUC, and by MALDI-TOF MS for the resulting IFNK31N_3 bioconjugates.

Method	SEC (kDa, Đ)	AUC (kDa)	MALDI-TOF MS (kDa)		AUC (kDa)	
Sample	Polymer	Polymer	Bioconjugate or protein	Bioconjugate - protein *	Bioconjugate or protein**	Bioconjugate - protein***
PEG 10 kDa	10.0, 1.04 [49]	7.9	30.3 [49]	10.7 [49]	27.7	8.0
PEG 20 kDa	23.3, 1.04 [a]	14.9	40.5	21.0	---	---
PEG 40 kDa	40, 1.08 [a]	47.6	60.2	40.7	---	---
LPG 10 kDa	11.6, 1.23 [49]	9.0	32.0 [49]	11.4 [49]	30.4	10.7
LPG 20 kDa	22.1, 1.22 [b]	19.8	44.6	25.1	---	---
LPG 40 kDa	54.8, 1.5 [b]	37.8	n.d.	n.d.	---	---
IFNK31N_3	---	---	19.5 [49]	---	19.7	---

[a] M_p according to manufacturer, [b] measured in H_2O by SEC calibrated with pullulan standards. *MW of IFNK31N_3(= 19.5 kDa) analyzed by MALDI-TOF MS was subtracted. **Average from RI and absorbance detection. *** MW of IFNK31N_3 analyzed by AUC (19.7 kDa**) was subtracted. [49] the value was published previously in the indicated reference. n.d. = not determinable

Conjugation, purification, and analysis of bioconjugates

Sedimentation-diffusion analysis, c(*s*), of IFNK31N_3 displayed a major species and a second less abundant species, both identified by data from the interference and absorbance detection module. The sedimentation coefficient for the monomer from both detector principles averaged to *s* = 1.95 S (**Figure 1E and S4D, Table S2**), which is in agreement with a recent study of recombinant human IFN-α2a in a nonrelated study[71]. Average molecular weights were calculated to be 19.7 kDa as an average based on absorbance and RI detection (**Tables 1 and S2**), comparable to the MALDI-TOF MS results. Next to the IFNK31N_3 monomer, the second species at *s*-values of ca.

2.8 S, presumably originates from a discernable existence of reversibly associated protein dimers, which has been reported previously for IFN-α2 at neutral pH [71, 72]. The BCN functionalized polymers were conjugated with azide functionalized IFN-α2a ($IFNK31N_3$; **Scheme 2**) and purified by FPLC (**Figure S5, Table S3**).

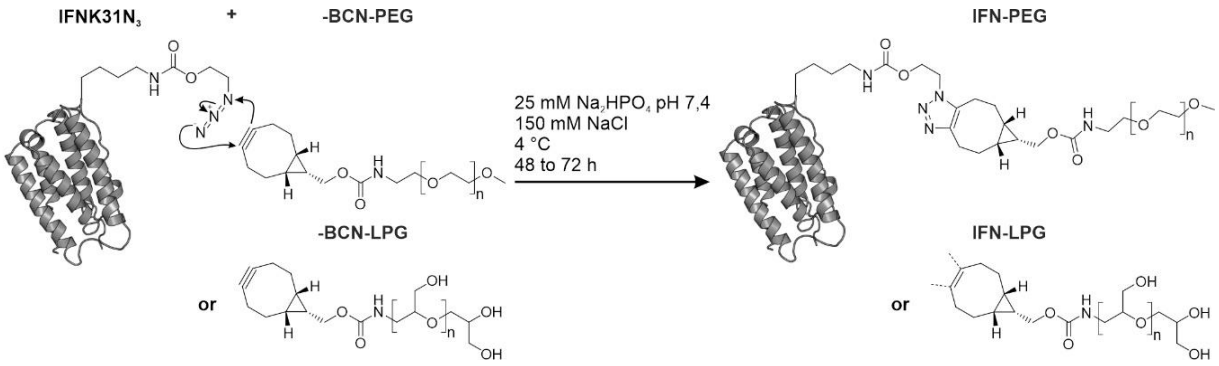

Scheme 2: Schematic representation of the BCN functionalized polymer conjugation to $IFNK31N_3$.

The product yield decreased with increasing molecular weight of the polymer (**Figure S5, Table S3**). The higher dispersity of LPG polymers reduced the collected fractions and, hence, lowered the yield (**Figure S5, Table S3**). The resulting molecular weights of 20 and 40 kDa PEG and 20 kDa LPG bioconjugates were confirmed by MALDI-TOF MS. The LPG 40 kDa bioconjugate could not be measured by MALDI-TOF MS, possibly reflecting its higher dispersity (**Figure S6, Table 1**). The calculated molecular weights of the conjugated polymers were in good agreement with SEC outcome after subtracting the mass of $IFNK31N_3$ from the measured mass of the bioconjugate, via MALDI-TOF MS, or AUC. Calculated molecular weights from AUC had the same tendency to slightly lower molecular weights, as did the sole polymers. SDS-PAGE analysis resulted in defined single bands for $IFNK31N_3$, IFN-α2a WT, and all bioconjugates except for the 40 kDa LPG (**Figures 2A, B**).

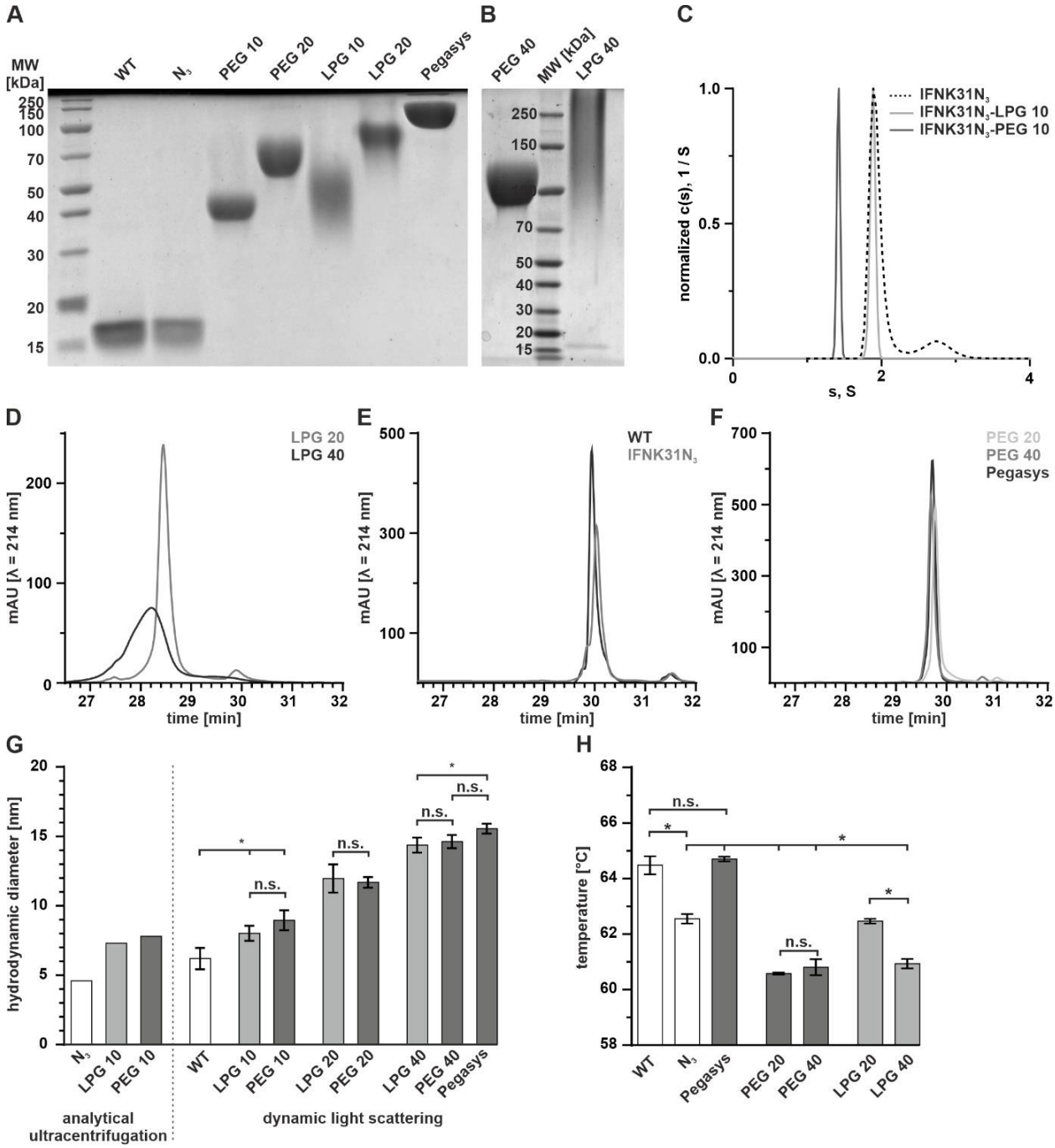

Figure 2: SDS-PAGE of (A) IFN-α2a WT (WT), IFNK31N_3 (N_3), IFNK31N_3-PEG 10 kDa (PEG 10), IFNK31N_3-PEG 20 kDa (PEG 20), IFNK31N_3-LPG 10 kDa (LPG 10), IFNK31N_3-LPG 20 kDa (LPG 20) and Pegasys, (B) IFNK31N_3-PEG 40 kDa (PEG 40) and IFNK31N_3-LPG 40 kDa (LPG40). (C) Normalized differential distributions of sedimentation coefficients, c(*s*), of 10 kDa bioconjugates by absorbance detection in terms of OD at λ = 280 nm (c(*s*) of IFNK31N_3, which is displayed in Figure 1E is displayed again for comparative purposes). Magnification of RP-HPLC chromatograms of (D) LPG-bioconjugates, (E) IFN-α2a WT and IFNK31N_3 and (F) PEG-bioconjugates (for full chromatograms please see Figure S7). (G) Hydrodynamic diameter of IFN-α2a WT and its bioconjugates (AUC n = 1; DLS n = 3; mean ± standard deviation; analysis for differences by one-sided ANOVA test followed by Tukey *post hoc* test for pair-wise comparison; $p < 0.05$ was considered statistically significant and selected differences as relevant for this study were marked by asterisks). (H) Melting points of bioconjugates determined by differential scanning fluorimetry (n ≥ 4; mean ± standard deviation; one-sided ANOVA test followed by Tukey *post hoc* test for pair-wise comparison; $p < 0.05$ was considered statistically significant and selected differences as relevant for this study were marked by asterisks).

The 40 kDa LPGylated bioconjugate was less defined (**Figure 2B**), which was further reflected by its broader peak in the HPLC chromatogram (**Figures 2D, S7**). Furthermore, bioconjugation increased the hydrophilicity of PEG and LPG bioconjugates when compared to the IFNK31N_3 mutant. This effect was more pronounced for the LPG conjugate than for the PEG conjugate (**Figure 2D-F, S7**).

Additionally, the 10 kDa PEG and LPG bioconjugates were analyzed by AUC (**Figure 2C and S4D**). The conjugation of PEG reduced the sedimentation velocity of the conjugate when compared to the protein monomer (despite higher overall molecular weights), resulting in a sedimentation coefficient of 1.42 *S*. The conjugation of LPG appeared not to significantly change the sedimentation velocity of the conjugate when compared to the protein monomer (despite higher overall molecular weights). It only led to a slight decrease to a sedimentation coefficient of 1.87 *S*. The conjugation of PEG and LPG to IFNK31N_3 did not show an apparent indication of dimers or higher aggregates, likely an effect of the polymeric stealth entity (**Figures 1E, 2C and S4D**). Data based on universal RI detection indicate the absence of free polymer while absorbance detection data are coherent with RI detection data for the conjugate (**Figure S4D**). Associated to sedimentation-diffusion analysis, we realized that the conjugated polymer (though of lower molecular weight than the protein) translated its much larger translational frictional properties to the protein, i.e., the biologic (**Table S2**). Calculated molecular weights for the protein and conjugates by sedimentation-diffusion analysis, c(*s*), followed the anticipations of conjugation and from MALDI-TOF MS. Again, the deceleration of the PEG conjugates compared to the protein, despite their higher molecular weights compared to the protein, is known in the scientific literature,[63, 73-75] also coined as a “parachute” like effect. Apparently, this effect is much reduced when using LPG conjugation as indicated here, though still being present. Bioconjugation

significantly increased the hydrodynamic diameter of the IFNK31N_3 mutant for all polymers as observed by dynamic light scattering (DLS) and calculated from AUC data, i.e., the polymer contributes pronouncedly to the measured and calculated hydrodynamic equivalent spherical size estimates (**Figure 2G, Table S4**). DLS and AUC data correlating to each other, as exemplarily compared for IFN-α2a itself and the 10 kDa bioconjugates of PEG and LPG, respectively. The LPG and PEG polymers had overall comparable sizes among the 10, 20 or 40 kDa polymer group. The hydrodynamic diameter of the PEG 40 kDa bioconjugates was comparable to the Pegasys conjugates, in contrast to all other bioconjugates which were smaller in hydrodynamic equivalent spherical size estimates. The unfolding temperature of all bioconjugates was comparable for all bioconjugates and significantly reduced as compared to IFN-α2a-WT, or Pegasys (**Figure 2H, S8, Table S4**).

Potency of bioconjugates

All bioconjugates had reduced potency as compared to IFN-α2a WT or the IFNK31N_3 mutant (**Figures 3A, S9, Table S4**) and bioconjugates performed similar within groups, and significantly different between groups of 10, 20, and 40 kDa bioconjugates. All groups performed significantly better than Pegasys. In general, an increasing hydrodynamic diameter inversely correlated with potency regardless of the polymer class used for conjugation following, *e.g.*, a third order polynomial regression for all conjugates other than Pegasys (**Figure 3B**).

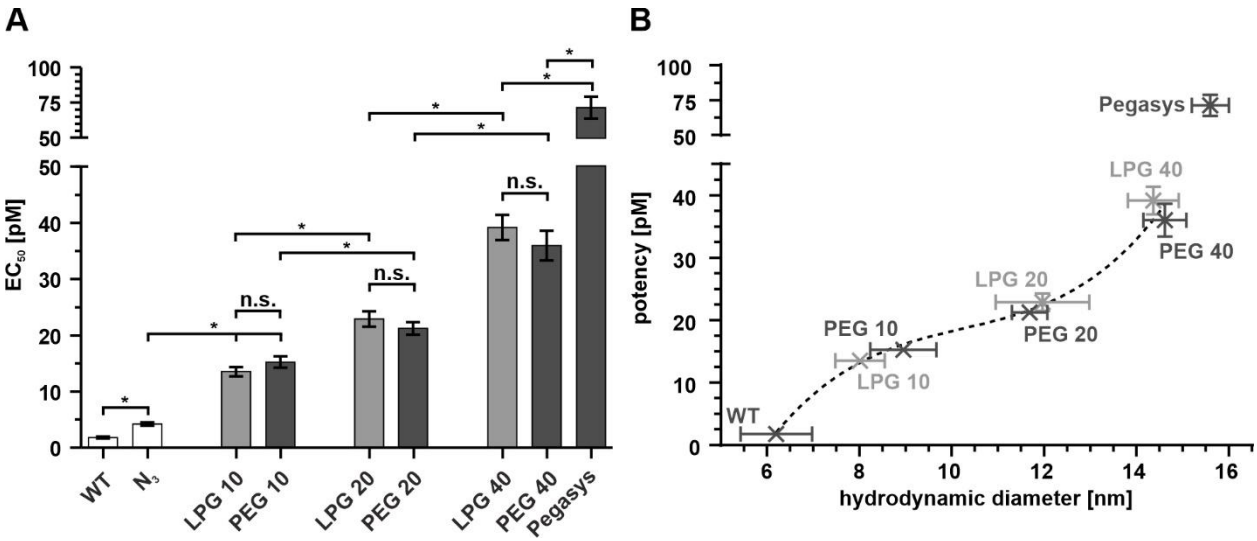

Figure 3: (A) EC_{50} values of bioconjugates ($n \geq 3$; mean ± standard deviation; analysis for differences by one-sided ANOVA test followed by Tukey *post hoc* test for pair-wise comparison; $p < 0.05$ was considered statistically significant and selected differences as relevant for this study were marked by asterisks. (B) Correlation of hydrodynamic diameter (data taken from Figure 2G) and potency (data taken from panel A of this figure).

Pharmacokinetics

IFN-α2a WT and all bioconjugates were stable in plasma throughout 48 hours (**Figure S10**). We further confirmed human IFN-α2a binding to the murine Interferon receptors by Fluorescence-Activated Cell Sorting (FACS) analysis of primary murine bone marrow cells (**Figure S11**). Resulting *in vivo* pharmacokinetics (PK) were mono-exponential for human IFN-α2a WT and PEG 20 kDa, and biphasic for all other bioconjugates. PK profiles for the human IFN-α2a WT were characterized by rapid disposition with a slope of about 9 h^{-1} ($t_{1/2} \approx 4$ min). The slope of the initial (distribution) phase indicated substantially slower distribution for the 20 kDa and 40 kDa LPG bioconjugates with 1.3 h^{-1} ($t_{1/2} \approx 32$ min) and 1.1 h^{-1} ($t_{1/2} \approx 39$ min), respectively, as compared to the wild type (**Figure 4, Tables S5-S7**). The distribution pharmacokinetics of the PEGylated bioconjugates and Pegasys was in the range of several hours, ranging from 0.2 to 0.14 h^{-1} ($t_{1/2} \approx 3$ h to 6 h). Terminal half-lives were some minutes for the IFN-α2a WT, and clustered between 2 hours and 4 hours for all 20 kDa bioconjugates. Substantially longer half-lives were recorded for

the LPG 40 kDa, Pegasys, and PEG 40 kDa bioconjugates with 14, 19, and 25 hours, respectively. Despite the rapid initial disposition of the LPG bioconjugates as compared to the PEGylated bioconjugates, resulting overall exposure (area under the curve) was in the same order of magnitude for LPG 40 kDa and Pegasys and both were lower than the PEG 40 kDa bioconjugates.

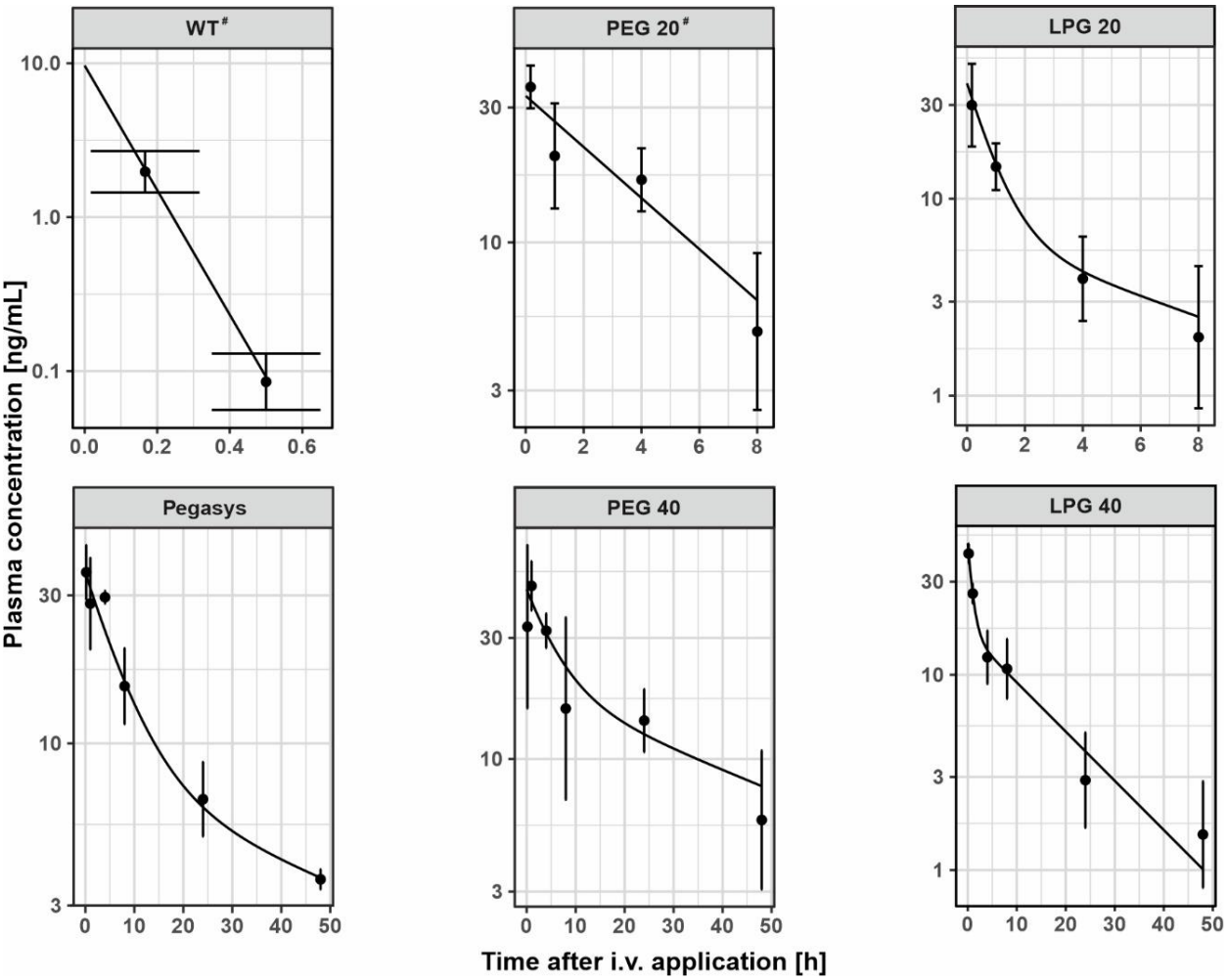

Figure 4: Pharmacokinetics of the human IFN-α2a WT and its bioconjugates (mean ± standard deviation, n ≥ 4). Mono-exponential pharmacokinetic were found for the human IFN-α2a WT and PEG 20 bioconjugate, respectively, and highlighted by a hashtag. All other profiles followed a biphasic pattern.

A faster distribution rate constant of LPGylated bioconjugates as compared to PEGylated bioconjugates was found although they had comparable hydrodynamic diameters (**Figure 5**).

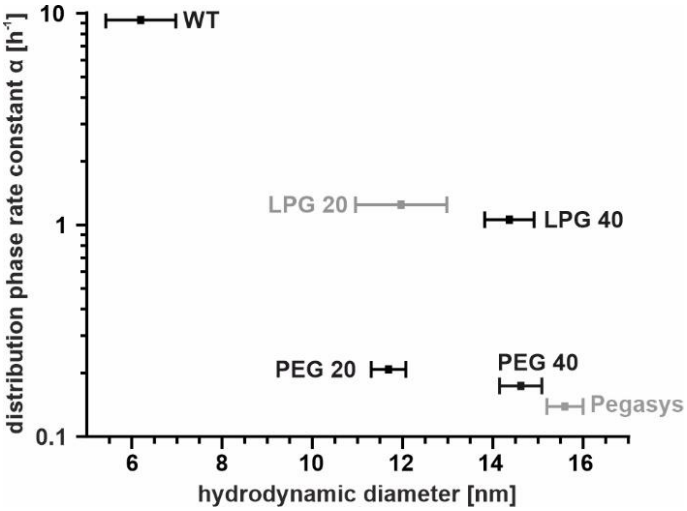

Figure 5: Hydrodynamic diameter (taken from Figure 2H, Table S4) and the initial rate/distribution rate constant (taken from Table S5). The PEG20 bioconjugate group followed mono-exponential kinetics (i.e. no distribution phase was distinguished).

Discussion

IFN-α2a mutants with a genetically introduced unnatural azide-carrying amino acid (IFNK31N_3) were manufactured and successfully conjugated with poly(ethylene glycol) (PEG) and linear polyglycerol (LPG) each with molecular weights of 20 or about 40 kDa (**Figure 2**). All bioconjugates had reduced potency as compared to IFN-α2a WT and its mutant, but higher potency as compared to the commercial product, Pegasys. The hydrodynamic diameter of the conjugates, but not their chemical nature negatively correlated with potency (**Figure 3**). Overall exposure of the 40 kDa PEG and 40 kDa LPG bioconjugates exceeded or matched those seen for Pegasys. A faster initial disposition was observed for the LPGylated bioconjugates as compared to the PEGylated bioconjugates, respectively, in spite of comparable hydrodynamic diameters (**Figure 5**).

Pegasys, among the first PEGylated biologics on the market, was selected as an exemplary starting point for systematically expanding the polymer space for cytokine bioconjugates [49]. A recent

publication using the same polymers with lower molecular weight, detailed optimal chemical linker structures between the biologic and the polymers as well as interaction patterns of the polymer-biologic interface [49]. This study now translates these findings to polymers with molecular weights targeting the colloidal dimensions of Pegasys and as required to lastingly modulate IFN-α2a pharmacokinetics for therapeutic use. The outcome reported here for IFN-α2a and Pegasys was in line with previous results from experiments with mice and rats [10, 21, 76, 77]. Interestingly, the LPGylated bioconjugates had a faster initial disposition as compared to the PEGylated counterparts with otherwise comparable hydrodynamic radii and potency (**Figure 3**). This provided evidence that these differences were not related to renal excretion. Furthermore, binding to serum components cannot explain these differences as supporting earlier reports indicate that albumin binding was not different for similar sized PEGylated or LPGylated human Interleukin-4 [50]. Hence, these differences in disposition kinetics are likely reflecting different distribution characteristics for LPGylated bioconjugates as compared to PEGylated bioconjugates. Interestingly, these at present unknown sinks for LPGylated bioconjugates were rapidly saturated such that overall exposure was not substantially impacted as compared to their PEGylated counterparts. Further studies are required to detail these findings, *e.g.*, comparing uptake phenomena in the liver or spleen for LPGylated and PEGylated bioconjugates and possibly binding studies in whole blood can detail potential binding to cellular components during circulation. Detailing these findings might in fact be particularly interesting for IFN-α2a bioconjugates. For example, previous studies indicated that prolonged exposure, as seen for Pegasys in comparison to the unconjugated wild type, shifted elimination from renal excretion to hepatic elimination [6]. Hence, different elimination routes may result from different polymers used for bioconjugation.

Similar outcome was obtained for the molecular weights of the polymers by SEC, AUC, and MALDI-TOF MS. While being in the same order of magnitude (**Table 1**), AUC analysis, though being performed from a limited amount of measurements, resulted in smaller molecular weights of the polymers, except for PEG 40 kDa. These effects were also found when calculating the molecular weight of the polymers by subtracting the mass of the protein from the AUC analysis outcome for the respective bioconjugates. Furthermore, the calculated and measured molecular weights of the bioconjugates by AUC and MALDI-TOF MS were not contrasting each other. An interesting aspect found in the sedimentation velocity data was re-affirmation of a "parachute" like effect on protein hydrodynamics for PEG conjugates,[63, 73, 74] observed also for LPG conjugates, but according to our present results to a much lower extend. This effect was coined down to originate from increased translational frictional ratios, f/f_{sph}, templated from the synthetic polymers on the biologic. Notwithstanding, AUC data unveiled rather accurate calculation of molecular weights of bioconjugates, since the methods of hydrodynamics inherently consider variations of translational friction properties associated to sedimentation and diffusion (the latter through translational frictional ratios, f/f_{sph}) in molecular weight estimations [75].

Potency negatively correlated with the hydrodynamic parameter (doubling diameter approximately reduced the potency four-fold; **Figure 3**) and was qualitatively reported for 10 kDa polymers before [49]. Nevertheless, melting temperature, which is regularly used as a predictor of secondary structure stability, was identical for Pegasys and IFN-α2a and in the range of previously reported results [49, 78]. The IFNK31N_3 mutant had significantly lower melting temperatures than IFN-α2a as had all other bioconjugates except for the LPG 20 kDa bioconjugate which had a melting temperature similar to the IFNK31N_3 mutant (**Figure 2H**). The data set does not allow to assess possible confounding effects of (i) shifting from IFN-α2a (Peagsys) to the IFNK31N_3

mutant (all other bioconjugates reported here), (ii) site directed conjugation or random conjugation (a total of eight lysines is target for random PEGylation in Pegasys; **Figure S12**), or (iii) polymer choice. However, the differences in melting temperature may be put into perspective with respect to previous studies by others. For example, the thermal stability of IFN-α2b at neutral pH could be improved by 2.6 °C just by changing the protein concentration and by 2.2 °C at increasing the ionic strength of the formulation [78]. To which extent these small differences are pharmaceutically relevant requires further real-time stability studies.

Conclusion

In conclusion, LPGylation is complementing bioconjugation possibilities beyond PEGylation with similar outcome in terms of the stability of the secondary structure (melting temperatures), and potency. Site specific polymer attachment may further increase the quality of the resulting bioconjugates. Differences were observed in terms of the pharmacokinetics, with faster initial distribution being observed for LPGylated as compared to PEGylated variants. At present the cause of these differences is unclear, but may point to LPG specific targeting mechanisms, possibly distinguishing this polymer from PEG.

Acknowledgements

We acknowledge the help of Dr. Andreas Schlosser, Juliane Adelmann, and Antje Gerlinde Heckmann with mass spectrometry and Nicole Bader with differential scanning fluorimetry assays (University of Würzburg). We further acknowledge Prof. Dr. Edward A. Lemke from the Johannes Gutenberg University of Mainz / EMBL Heidelberg for donating the pEVOL-pylRS vector. We further thank the Core Facility BioSupraMol for NMR measurements, Daniel Kutifa for assistance with polymerization reactions and Cathleen Hudziak for SEC measurements (Freie Universität

Berlin). The project was funded within the framework ‘Next-PEG’ by the Federal Ministry of Education and Research (BMBF) of Germany (# 13XP5049), the “Thüringer Aufbaubank (TAB)”, and the “Europäischer Fonds für regionale Entwicklung (EFRE)” (2018FGI0025). G.C. acknowledges support from the Free State of Thuringia and the European Social Fund (2019SD0129).

Supporting Information

Supporting results include results of size exclusion chromatography, NMR of polymers, additional AUC results, full chromatograms of RP-HPLC analysis, SDS-PAGE of 20 and 40 kDa bioconjugate purifications, MALDI-TOF MS results, potency stimulation curves, additional DSF data, results of human plasma stability and FACS analysis of IFN-α2a stimulated murine bone marrow cells.

Author Information

Corresponding author

Prof. Dr. Dr. Lorenz Meinel, Institute of Pharmacy and Food Chemistry, University of Würzburg, Am Hubland, DE-97074 Würzburg, Germany, lorenz.meinel@uni-wuerzburg.de, Tel.: +49 931 3185471

Notes

N.Hauptstein and P. Pouyan have contributed equally to this work.

Declaration of interest

None

References

[1] A. Abuchowski, J.R. McCoy, N.C. Palczuk, T. van Es, F.F. Davis, Effect of covalent attachment of polyethylene glycol on immunogenicity and circulating life of bovine liver catalase, J. Biol. Chem., 252 (1977) 3582-3586.
[2] A. Abuchowski, T. van Es, N.C. Palczuk, F.F. Davis, Alteration of immunological properties of bovine serum albumin by covalent attachment of polyethylene glycol, J. Biol. Chem., 252 (1977) 3578-3581.
[3] P. Bastard, L.B. Rosen, Q. Zhang, E. Michailidis, H.-H. Hoffmann, Y. Zhang, K. Dorgham, Q. Philippot, J. Rosain, V. Béziat, J. Manry, E. Shaw, L. Haljasmägi, P. Peterson, L. Lorenzo, L. Bizien, S. Trouillet-Assant, K. Dobbs, A.A. de Jesus, A. Belot, A. Kallaste, E. Catherinot, Y. Tandjaoui-Lambiotte, J. Le Pen, G. Kerner, B. Bigio, Y. Seeleuthner, R. Yang, A. Bolze, A.N. Spaan, O.M. Delmonte, M.S. Abers, A. Aiuti, G. Casari, V. Lampasona, L. Piemonti, F. Ciceri, K. Bilguvar, R.P. Lifton, M. Vasse, D.M. Smadja, M. Migaud, J. Hadjadj, B. Terrier, D. Duffy, L. Quintana-Murci, D. van de Beek, L. Roussel, D.C. Vinh, S.G. Tangye, F. Haerynck, D. Dalmau, J. Martinez-Picado, P. Brodin, M.C. Nussenzweig, S. Boisson-Dupuis, C. Rodríguez-Gallego, G. Vogt, T.H. Mogensen, A.J. Oler, J. Gu, P.D. Burbelo, J.I. Cohen, A. Biondi, L.R. Bettini, M. D'Angio, P. Bonfanti, P. Rossignol, J. Mayaux, F. Rieux-Laucat, E.S. Husebye, F. Fusco, M.V. Ursini, L. Imberti, A. Sottini, S. Paghera, E. Quiros-Roldan, C. Rossi, R. Castagnoli, D. Montagna, A. Licari, G.L. Marseglia, X. Duval, J. Ghosn, J.S. Tsang, R. Goldbach-Mansky, K. Kisand, M.S. Lionakis, A. Puel, S.-Y. Zhang, S.M. Holland, G. Gorochov, E. Jouanguy, C.M. Rice, A. Cobat, L.D. Notarangelo, L. Abel, H.C. Su, J.-L. Casanova, Autoantibodies against type I IFNs in patients with life-threatening COVID-19, Science, 370 (2020) eabd4585.
[4] J.M. Harris, R.B. Chess, Effect of pegylation on pharmaceuticals, Nat. Rev. Drug Discov., 2 (2003) 214-221.
[5] K. Knop, R. Hoogenboom, D. Fischer, U.S. Schubert, Poly(ethylene glycol) in Drug Delivery: Pros and Cons as Well as Potential Alternatives, Angew. Chem. Int. Ed., 49 (2010) 6288-6308.
[6] P. Glue, J.W. Fang, R. Rouzier-Panis, C. Raffanel, R. Sabo, S.K. Gupta, M. Salfi, S. Jacobs, Pegylated interferon-alpha2b: pharmacokinetics, pharmacodynamics, safety, and preliminary efficacy data. Hepatitis C Intervention Therapy Group, Clin. Pharmacol. Ther., 68 (2000) 556-567.
[7] S. Zeuzem, C. Welsch, E. Herrmann, Pharmacokinetics of peginterferons, Semin. Liver Dis., 23 Suppl 1 (2003) 23-28.
[8] E.C. Borden, G.C. Sen, G. Uze, R.H. Silverman, R.M. Ransohoff, G.R. Foster, G.R. Stark, Interferons at age 50: past, current and future impact on biomedicine, Nat. Rev. Drug Discov., 6 (2007) 975-990.
[9] S.-J. Hsu, M.-L. Yu, C.-W. Su, C.-Y. Peng, R.-N. Chien, H.-H. Lin, G.-H. Lo, W.-W. Su, H.-T. Kuo, C.-W. Hsu, S.-S. Yang, S.-S. Yang, K.-C. Tseng, A. Qin, Y.-W. Huang, W.-L. Chuang, Ropeginterferon Alfa-2b administered every two weeks for patients with genotype 2 chronic hepatitis C, J. Formosan Med. Assoc., (2020).
[10] V.M. McLeod, L.J. Chan, G.M. Ryan, C.J. Porter, L.M. Kaminskas, Optimal PEGylation can improve the exposure of interferon in the lungs following pulmonary administration, J. Pharm. Sci., 104 (2015) 1421-1430.
[11] R. Perrillo, Benefits and risks of interferon therapy for hepatitis B, Hepatology, 49 (2009) S103-111.
[12] J. Piehler, C. Thomas, K.C. Garcia, G. Schreiber, Structural and dynamic determinants of type I interferon receptor assembly and their functional interpretation, Immunol. Rev., 250 (2012) 317-334.
[13] K. Rajender Reddy, M.W. Modi, S. Pedder, Use of peginterferon alfa-2a (40 KD) (Pegasys®) for the treatment of hepatitis C, Adv. Drug Del. Rev., 54 (2002) 571-586.
[14] A.T. Reder, X. Feng, How type I interferons work in multiple sclerosis and other diseases: some unexpected mechanisms, J. Interferon Cytokine Res., 34 (2014) 589-599.

[15] M.S. Rosendahl, D.H. Doherty, D.J. Smith, S.J. Carlson, E.A. Chlipala, G.N. Cox, A Long-Acting, Highly Potent Interferon α-2 Conjugate Created Using Site-Specific PEGylation, Bioconjugate Chem., 16 (2005) 200-207.
[16] L.M. Snell, T.L. McGaha, D.G. Brooks, Type I Interferon in Chronic Virus Infection and Cancer, Trends Immunol., 38 (2017) 542-557.
[17] C. Thomas, I. Moraga, D. Levin, P.O. Krutzik, Y. Podoplelova, A. Trejo, C. Lee, G. Yarden, S.E. Vleck, J.S. Glenn, G.P. Nolan, J. Piehler, G. Schreiber, K.C. Garcia, Structural linkage between ligand discrimination and receptor activation by type I interferons, Cell, 146 (2011) 621-632.
[18] M. Uchihara, N. Izumi, Y. Sakai, T. Yauchi, S. Miyake, T. Sakai, T. Akiba, F. Marumo, C. Sato, Interferon Therapy for Chronic Hepatitis C in Hemodialysis Patients: Increased Serum Levels of Interferon, Nephron, 80 (1998) 51-56.
[19] Y.-S. Wang, S. Youngster, M. Grace, J. Bausch, R. Bordens, D.F. Wyss, Structural and biological characterization of pegylated recombinant interferon alpha-2b and its therapeutic implications, Adv. Drug Del. Rev., 54 (2002) 547-570.
[20] Y.S. Wang, S. Youngster, J. Bausch, R. Zhang, C. McNemar, D.F. Wyss, Identification of the major positional isomer of pegylated interferon alpha-2b, Biochemistry, 39 (2000) 10634-10640.
[21] P. Bailon, A. Palleroni, C.A. Schaffer, C.L. Spence, W.J. Fung, J.E. Porter, G.K. Ehrlich, W. Pan, Z.X. Xu, M.W. Modi, A. Farid, W. Berthold, M. Graves, Rational design of a potent, long-lasting form of interferon: a 40 kDa branched polyethylene glycol-conjugated interferon alpha-2a for the treatment of hepatitis C, Bioconjug Chem, 12 (2001) 195-202.
[22] EMA, Pegasys 180 micrograms solution for injection https://www.ema.europa.eu/en/documents/product-information/pegasys-epar-product-information_en.pdf, accessed November 2021.
[23] EMA, PegIntron 50 micrograms powder and solvent for solution for injection https://ec.europa.eu/health/documents/community-register/2016/20160629135304/anx_135304_en.pdf, accessed November 2021.
[24] EMA, Besremi 250 micrograms/0.5 mL solution for injection in pre-filled pen https://www.ema.europa.eu/en/documents/product-information/besremi-epar-product-information_en.pdf, accessed November 2021.
[25] G.T. Kozma, T. Shimizu, T. Ishida, J. Szebeni, Anti-PEG antibodies: Properties, formation, testing and role in adverse immune reactions to PEGylated nano-biopharmaceuticals, Adv. Drug Del. Rev., 154-155 (2020) 163-175.
[26] N.E. Elsadek, A.S. Abu Lila, T. Ishida, 5 - Immunological responses to PEGylated proteins: anti-PEG antibodies, in: G. Pasut, S. Zalipsky (Eds.) Polymer-Protein Conjugates, Elsevier, 2020, pp. 103-123.
[27] S. Foser, A. Schacher, K.A. Weyer, D. Brugger, E. Dietel, S. Marti, T. Schreitmüller, Isolation, structural characterization, and antiviral activity of positional isomers of monopegylated interferon α-2a (PEGASYS), Protein Expression Purif., 30 (2003) 78-87.
[28] Q. Yang, S.K. Lai, Anti-PEG immunity: emergence, characteristics, and unaddressed questions, WIREs Nanomed Nanobiotechnol, 7 (2015) 655-677.
[29] J.A. Shadish, C.A. DeForest, Site-Selective Protein Modification: From Functionalized Proteins to Functional Biomaterials, Matter, 2 (2020) 50-77.
[30] I. Ekladious, Y.L. Colson, M.W. Grinstaff, Polymer–drug conjugate therapeutics: advances, insights and prospects, Nat. Rev. Drug Discov., 18 (2019) 273-294.
[31] T. Lühmann, L. Meinel, Nanotransporters for drug delivery, Curr. Opin. Biotechnol., 39 (2016) 35-40.
[32] A.C. Braun, M. Gutmann, R. Ebert, F. Jakob, H. Gieseler, T. Lühmann, L. Meinel, Matrix Metalloproteinase Responsive Delivery of Myostatin Inhibitors, Pharm. Res., 34 (2017) 58-72.
[33] A.C. Braun, M. Gutmann, T.D. Mueller, T. Lühmann, L. Meinel, Bioresponsive release of insulin-like growth factor-I from its PEGylated conjugate, J. Controlled Release, 279 (2018) 17-28.

[34] K. Dodt, S. Lamer, M. Drießen, S. Bölch, A. Schlosser, T. Lühmann, L. Meinel, Mass-Encoded Reporters Reporting Proteolytic Activity from within the Extracellular Matrix, ACS Biomater. Sci. Eng., 6 (2020) 5240-5253.
[35] K. Dodt, M.D. Driessen, S. Lamer, A. Schlosser, T. Lühmann, L. Meinel, A Complete and Versatile Protocol: Decoration of Cell-Derived Matrices with Mass-Encoded Peptides for Multiplexed Protease Activity Detection, ACS Biomater. Sci. Eng., 6 (2020) 6598-6617.
[36] T. Lühmann, G. Jones, M. Gutmann, J.-C. Rybak, J. Nickel, M. Rubini, L. Meinel, Bio-orthogonal Immobilization of Fibroblast Growth Factor 2 for Spatial Controlled Cell Proliferation, ACS Biomater. Sci. Eng., 1 (2015) 740-746.
[37] H. Zhao, E. Heusler, G. Jones, L. Li, V. Werner, O. Germershaus, J. Ritzer, T. Luehmann, L. Meinel, Decoration of silk fibroin by click chemistry for biomedical application, J. Struct. Biol., 186 (2014) 420-430.
[38] M. Gutmann, E. Memmel, A.C. Braun, J. Seibel, L. Meinel, T. Lühmann, Biocompatible Azide–Alkyne "Click" Reactions for Surface Decoration of Glyco-Engineered Cells, ChemBioChem, 17 (2016) 866-875.
[39] T. Lühmann, V. Spieler, V. Werner, M.-G. Ludwig, J. Fiebig, T.D. Mueller, L. Meinel, Interleukin-4-Clicked Surfaces Drive M2 Macrophage Polarization, ChemBioChem, 17 (2016) 2123-2128.
[40] G. Wandrey, J. Wurzel, K. Hoffmann, T. Ladner, J. Büchs, L. Meinel, T. Lühmann, Probing unnatural amino acid integration into enhanced green fluorescent protein by genetic code expansion with a high-throughput screening platform, J. Biol. Eng., 10 (2016) 11.
[41] T. Lühmann, M. Schmidt, M.N. Leiske, V. Spieler, T.C. Majdanski, M. Grube, M. Hartlieb, I. Nischang, S. Schubert, U.S. Schubert, L. Meinel, Site-Specific POxylation of Interleukin-4, ACS Biomater. Sci. Eng., 3 (2017) 304-312.
[42] C. Siverino, B. Tabisz, T. Lühmann, L. Meinel, T. Müller, H. Walles, J. Nickel, Site-Directed Immobilization of Bone Morphogenetic Protein 2 to Solid Surfaces by Click Chemistry, J. Visualized Exp., (2018) 56616.
[43] F. Wu, A. Braun, T. Lühmann, L. Meinel, Site-Specific Conjugated Insulin-like Growth Factor-I for Anabolic Therapy, ACS Biomater. Sci. Eng., 4 (2018) 819-825.
[44] A.C. Braun, M. Gutmann, T. Lühmann, L. Meinel, Bioorthogonal strategies for site-directed decoration of biomaterials with therapeutic proteins, J. Controlled Release, 273 (2018) 68-85.
[45] A.C. Braun, M. Gutmann, T.D. Mueller, T. Lühmann, L. Meinel, Bioresponsive release of insulin-like growth factor-I from its PEGylated conjugate, J. Controlled Release, 279 (2018) 17–28.
[46] M. Gutmann, J. Bechold, J. Seibel, L. Meinel, T. Lühmann, Metabolic Glycoengineering of Cell-Derived Matrices and Cell Surfaces: A Combination of Key Principles and Step-by-Step Procedures, ACS Biomater. Sci. Eng., 5 (2019) 215-233.
[47] T. Lühmann, M. Gutmann, A. Moscaroli, M. Raschig, M. Béhé, L. Meinel, Biodistribution of Site-Specific PEGylated Fibroblast Growth Factor-2, ACS Biomater. Sci. Eng., 6 (2020) 425-432.
[48] V. Spieler, M.-G. Ludwig, J. Dawson, B. Tigani, A. Littlewood-Evans, C. Safina, H. Ebersbach, K. Seuwen, M. Raschig, B. ter Mors, T.D. Müller, L. Meinel, T. Lühmann, Targeting interleukin-4 to the arthritic joint, J. Controlled Release, 326 (2020) 172-180.
[49] N. Hauptstein, P. Pouyan, J. Kehrein, M. Dirauf, M.D. Driessen, M. Raschig, K. Licha, M. Gottschaldt, U.S. Schubert, R. Haag, L. Meinel, C. Sotriffer, T. Lühmann, Molecular Insights into Site-Specific Interferon-α2a Bioconjugates Originated from PEG, LPG, and PEtOx, Biomacromolecules, 22 (2021) 4521-4534.
[50] M. Tully, N. Hauptstein, K. Licha, L. Meinel, T. Lühmann, R. Haag, Linear Polyglycerol for N-terminal-selective Modification of Interleukin-4, J. Pharm. Sci., (2021).
[51] M. Tully, M. Dimde, C. Weise, P. Pouyan, K. Licha, M. Schirner, R. Haag, Polyglycerol for Half-Life Extension of Proteins—Alternative to PEGylation?, Biomacromolecules, 22 (2021) 1406-1416.

[52] M. Tully, S. Wedepohl, D. Kutifa, C. Weise, K. Licha, M. Schirner, R. Haag, Prolonged activity of exenatide: Detailed comparison of Site-specific linear polyglycerol- and poly(ethylene glycol)-conjugates, Eur. J. Pharm. Biopharm., 164 (2021) 105-113.
[53] E. Wenande, L.H. Garvey, Immediate-type hypersensitivity to polyethylene glycols: a review, Clin Exp Allergy, 46 (2016) 907-922.
[54] J. Pickert, I. Hennighausen, S. Mühlenbein, C. Möbs, W. Pfützner, Immediate-Type Hypersensitivity to Polyethylene Glycol (PEG) Including a PEG-containing COVID-19 Vaccine Revealed by Intradermal Testing, J. Investig. Allergol. Clin. Immunol., (2021) 0.
[55] J.T. Huckaby, T.M. Jacobs, Z. Li, R.J. Perna, A. Wang, N.I. Nicely, S.K. Lai, Structure of an anti-PEG antibody reveals an open ring that captures highly flexible PEG polymers, Commun. Chem., 3 (2020) 124.
[56] T.T. Hoang Thi, E.H. Pilkington, D.H. Nguyen, J.S. Lee, K.D. Park, N.P. Truong, The Importance of Poly(ethylene glycol) Alternatives for Overcoming PEG Immunogenicity in Drug Delivery and Bioconjugation, Polymers, 12 (2020).
[57] P. Schuck, Size-Distribution Analysis of Macromolecules by Sedimentation Velocity Ultracentrifugation and Lamm Equation Modeling, Biophys. J., 78 (2000) 1606-1619.
[58] P. Schuck, M.A. Perugini, N.R. Gonzales, G.J. Howlett, D. Schubert, Size-distribution analysis of proteins by analytical ultracentrifugation: strategies and application to model systems, Biophys. J., 82 (2002) 1096-1111.
[59] I. Nischang, I. Perevyazko, T. Majdanski, J. Vitz, G. Festag, U.S. Schubert, Hydrodynamic Analysis Resolves the Pharmaceutically-Relevant Absolute Molar Mass and Solution Properties of Synthetic Poly(ethylene glycol)s Created by Varying Initiation Sites, Anal. Chem., 89 (2017) 1185-1193.
[60] M. Grube, M.N. Leiske, U.S. Schubert, I. Nischang, POx as an Alternative to PEG? A Hydrodynamic and Light Scattering Study, Macromolecules, 51 (2018) 1905-1916.
[61] P.H. Brown, A. Balbo, H. Zhao, C. Ebel, P. Schuck, Density Contrast Sedimentation Velocity for the Determination of Protein Partial-Specific Volumes, PLoS One, 6 (2011) e26221.
[62] H. Durchschlag, Determination of the partial specific volume of conjugated proteins, Colloid. Polym. Sci., 267 (1989) 1139-1150.
[63] C. Dhalluin, A. Ross, L.-A. Leuthold, S. Foser, B. Gsell, F. Müller, H. Senn, Structural and Biophysical Characterization of the 40 kDa PEG−Interferon-α2a and Its Individual Positional Isomers, Bioconjugate Chem., 16 (2005) 504-517.
[64] C.D. Reinkemeier, E.A. Lemke, Raising the ribosomal repertoire, Nat. Chem., 12 (2020) 503-504.
[65] A. Borrmann, S. Milles, T. Plass, J. Dommerholt, J.M. Verkade, M. Wiessler, C. Schultz, J.C. van Hest, F.L. van Delft, E.A. Lemke, Genetic encoding of a bicyclo[6.1.0]nonyne-charged amino acid enables fast cellular protein imaging by metal-free ligation, Chembiochem, 13 (2012) 2094-2099.
[66] M. Tully, N. Hauptstein, K. Licha, L. Meinel, T. Lühmann, R. Haag, Linear Polyglycerol for N-terminal-selective Modification of Interleukin-4, J. Pharm. Sci., (2021).
[67] C. Sun, Y. Li, E.A. Yates, D.G. Fernig, SimpleDSFviewer: A tool to analyze and view differential scanning fluorimetry data for characterizing protein thermal stability and interactions, Protein Sci., 29 (2020) 19-27.
[68] M.G. Tovey, C. Lallemand, J.-F. Meritet, C. Maury, Adjuvant activity of interferon alpha: mechanism(s) of action, Vaccine, 24 (2006) S46-S47.
[69] K. Müller, here: A Simpler Way to Find Your Files. https://CRAN.R-project.org/package=here, accessed november 2021, (2020).
[70] P. Pouyan, C. Nie, S. Bhatia, S. Wedepohl, K. Achazi, N. Osterrieder, R. Haag, Inhibition of Herpes Simplex Virus Type 1 Attachment and Infection by Sulfated Polyglycerols with Different Architectures, Biomacromolecules, 22 (2021) 1545-1554.

[71] R.L. Bis, T.M. Stauffer, S.M. Singh, T.B. Lavoie, K.M.G. Mallela, High yield soluble bacterial expression and streamlined purification of recombinant human interferon α-2a, Protein Expression Purif., 99 (2014) 138-146.
[72] S.J. Shire, pH-dependent polymerization of a human leukocyte interferon produced by recombinant deoxyribonucleic acid technology, Biochemistry, 22 (1983) 2664-2671.
[73] Y. Lu, S.E. Harding, A. Turner, B. Smith, D.S. Athwal, J.G. Grossmann, K.G. Davis, A.J. Rowe, Effect of PEGylation on the Solution Conformation of Antibody Fragments, J. Pharm. Sci., 97 (2008) 2062-2079.
[74] Y.R. Gokarn, M. McLean, T.M. Laue, Effect of PEGylation on Protein Hydrodynamics, Mol. Pharm., 9 (2012) 762-773.
[75] O.J. Valderrama, I. Nischang, Reincarnation of the Analytical Ultracentrifuge: Emerging Opportunities for Nanomedicine, Anal. Chem., 93 (2021) 15805-15815.
[76] K.-J. Zhang, X.-F. Yin, Y.-Q. Yang, H.-L. Li, Y.-N. Xu, L.-Y. Chen, X.-J. Liu, S.-J. Yuan, X.-L. Fang, J. Xiao, S. Wu, H.-N. Xu, L. Chu, K.V. Katlinski, Y.V. Katlinskaya, R.-B. Guo, G.-W. Wei, D.-C. Wang, X.-Y. Liu, S.Y. Fuchs, A Potent *In Vivo* Antitumor Efficacy of Novel Recombinant Type I Interferon, Clin. Cancer Res., 23 (2017) 2038-2049.
[77] J. Hu, G. Wang, X. Liu, W. Gao, Enhancing Pharmacokinetics, Tumor Accumulation, and Antitumor Efficacy by Elastin-Like Polypeptide Fusion of Interferon Alpha, Adv. Mater., 27 (2015) 7320-7324.
[78] A. Beldarraín, Y. Cruz, O. Cruz, M. Navarro, M. Gil, Purification and conformational properties of a human interferon alpha2b produced in Escherichia coli, Biotechnol Appl Biochem, 33 (2001) 173-182.

for the Table of Contents use only

Polymer selection impacts the pharmaceutical profile of site specifically conjugated Interferon-α2a

Niklas Hauptstein, Paria Pouyan, Kevin Wittwer, Gizem Cinar, Oliver Scherf-Clavel, Martina Raschig, Kai Licha, Tessa Lühmann, Ivo Nischang, Ulrich S. Schubert, Christian Pfaller, Rainer Haag, Lorenz Meinel*

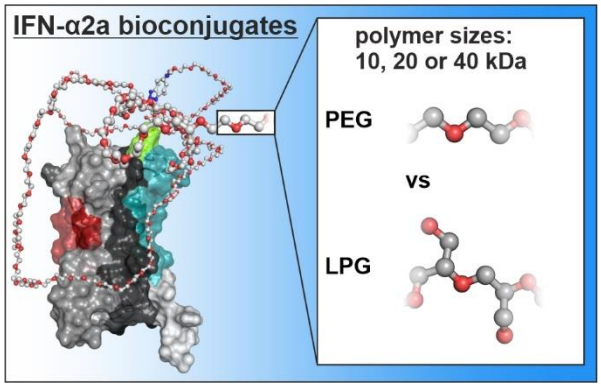

Site-specific conjugation of Interferon-α2a mutants to poly(ethylene glycol) or polyglycerol of about 10 kDa, 20 kDa or 40 kDa, respectively, impacted the distribution of resulting bioconjugates dependent on polymer choice.